

# Optical implementation and entanglement distribution in Gaussian valence bond states

**Gerardo Adesso**

Centre for Quantum Computation, DAMTP, Centre for Mathematical Sciences, University of Cambridge, Wilberforce Road, Cambridge CB3 0WA, United Kingdom;  
Dipartimento di Fisica, Università di Roma “La Sapienza”, Piazzale Aldo Moro 5, 00185 Roma, Italy;  
Dipartimento di Fisica “E. R. Caianiello”, Università degli Studi di Salerno, Via S. Allende, 84081 Baronissi (SA), Italy

**Marie Ericsson**

Centre for Quantum Computation, DAMTP, Centre for Mathematical Sciences, University of Cambridge, Wilberforce Road, Cambridge CB3 0WA, United Kingdom

PACS numbers: 42.50.Dv, 03.67.Mn, 03.67.Hk, 03.65.Ud.

**Abstract.** We study Gaussian valence bond states of continuous variable systems, obtained as the outputs of projection operations from an ancillary space of  $M$  infinitely entangled bonds connecting neighboring sites, applied at each of  $N$  sites of an harmonic chain. The entanglement distribution in Gaussian valence bond states can be controlled by varying the input amount of entanglement engineered in a  $(2M + 1)$ -mode Gaussian state known as the building block, which is isomorphic to the projector applied at a given site. We show how this mechanism can be interpreted in terms of multiple entanglement swapping from the chain of ancillary bonds, through the building blocks. We provide optical schemes to produce bisymmetric three-mode Gaussian building blocks (which correspond to a single bond,  $M = 1$ ), and study the entanglement structure in the output Gaussian valence bond states. The usefulness of such states for quantum communication protocols with continuous variables, like telecloning and teleportation networks, is finally discussed.

## 1. Introduction

Quantum information aims at the treatment and transport of information in ways forbidden by classical physics. For this goal, continuous variables (CV) of atoms and light have emerged as a powerful tool [1]. In this context, entanglement is an essential resource. Recently, the valence bond formalism, originally developed for spin systems [2], has been generalized to the CV scenario [3, 4] for the special class of Gaussian states, which play a central role in theoretical and practical CV quantum information and communication [5].

In this work we analyze feasible implementations of Gaussian valence bond states (GVBS) for quantum communication between many users in a CV setting, as enabled by their peculiar structure of distributed entanglement [4]. After recalling the necessary notation (Sec. 2) and the construction of Gaussian valence bond states [3] (Sec. 3), we discuss the characterization of entanglement and its distribution in such states as regulated by the entanglement properties of simpler states involved in the valence bond construction [4] (Sec. 4). We then focus on the realization of GVBS by means of quantum optics, provide a scheme for their state engineering (Sec. 5), and discuss the applications of such resources in the context of CV telecloning [6, 7] on multimode harmonic rings (Sec. 6).

## 2. Continuous variable systems and Gaussian states

A CV system [1, 5] is described by a Hilbert space  $\mathcal{H} = \bigotimes_{i=1}^N \mathcal{H}_i$  resulting from the tensor product of infinite dimensional Fock spaces  $\mathcal{H}_i$ 's. Let  $a_i$  and  $a_i^\dagger$  be the annihilation and creation operators acting on  $\mathcal{H}_i$  (ladder operators), and  $\hat{q}_i = (a_i + a_i^\dagger)/i$  and  $\hat{p}_i = (a_i - a_i^\dagger)$  be the related quadrature phase operators. Let  $\hat{R} = (\hat{x}_1, \hat{p}_1, \dots, \hat{q}_N, \hat{p}_N)$  denote the vector of the operators  $\hat{q}_i$  and  $\hat{p}_i$ . The canonical commutation relations for the  $\hat{R}_i$  can be expressed in terms of the symplectic form  $\Omega$  as

$$[\hat{R}_i, \hat{R}_j] = 2i\Omega_{ij} ,$$

$$\text{with } \Omega \equiv \omega^{\oplus N} , \quad \omega \equiv \begin{pmatrix} 0 & 1 \\ -1 & 0 \end{pmatrix} .$$

The state of a CV system can be equivalently described by quasi-probability distributions defined on the  $2N$ -dimensional space associated to the quadratic form  $\Omega$ , known as quantum *phase space*. In the phase space picture, the tensor product  $\mathcal{H} = \bigotimes_i^N \mathcal{H}_i$  of the Hilbert spaces  $\mathcal{H}_i$ 's of the  $N$  modes results in the direct sum  $\Lambda = \bigoplus_i^N \Lambda_i$  of the phase spaces  $\Lambda_i$ 's.

States with Gaussian quasi-probability distributions are referred to as *Gaussian states*. Such states are at the heart of information processing in CV systems [1, 5] and are the subject of our analysis. By definition, a Gaussian state is completely characterized by the first and second statistical moments of the field operators, which will be denoted, respectively, by the vector of first moments  $\bar{R} \equiv (\langle \hat{R}_1 \rangle, \langle \hat{R}_2 \rangle, \dots, \langle \hat{R}_{2N-1} \rangle, \langle \hat{R}_{2N} \rangle)$  and the covariance matrix (CM)  $\gamma$  of elements

$$\gamma_{ij} \equiv \frac{1}{2} \langle \hat{R}_i \hat{R}_j + \hat{R}_j \hat{R}_i \rangle - \langle \hat{R}_i \rangle \langle \hat{R}_j \rangle . \quad (1)$$

Coherent states, resulting from the application of displacement operators  $D_Y = e^{iY^T \Omega \hat{R}}$  ( $Y \in \mathbb{R}^{2n}$ ) to the vacuum state, are Gaussian states with CM  $\gamma = \mathbb{1}$  and first statistical moments  $\bar{R} = Y$ . First moments can be arbitrarily adjusted by local unitary operations (displacements), which cannot affect any property related to entropy or entanglement. They

can thus be assumed zero without any loss of generality. A  $N$ -mode Gaussian state will be completely characterized by its real, symmetric,  $2N \times 2N$  CM  $\gamma$ .

The canonical commutation relations and the positivity of the density matrix  $\rho$  of a Gaussian state imply the *bona fide* condition

$$\gamma + i\Omega \geq 0, \quad (2)$$

as a necessary and sufficient constraint the matrix  $\gamma$  has to fulfill to be a CM corresponding to a physical state [8, 9]. Note that the previous condition is necessary for the CM of *any* (generally non Gaussian) state, as it generalizes to many modes the Robertson-Schrödinger uncertainty relation [10].

A major role in the theoretical and experimental manipulation of Gaussian states is played by unitary operations which preserve the Gaussian character of the states on which they act. Such operations are all those generated by terms of the first and second order in the field operators. As a consequence of the Stone-Von Neumann theorem, any such operation at the Hilbert space level corresponds, in phase space, to a symplectic transformation, i.e. to a linear transformation  $S$  which preserves the symplectic form  $\Omega$ , so that  $\Omega = S^T \Omega S$ , i.e. it preserves the commutators between the different operators. Symplectic transformations on a  $2N$ -dimensional phase space form the (real) symplectic group, denoted by  $Sp_{(2N, \mathbb{R})}$ . Such transformations act linearly on first moments and “by congruence” on the CM (i.e. so that  $\gamma \mapsto S\gamma S^T$ ). One has  $\text{Det } S = 1, \forall S \in Sp_{(2N, \mathbb{R})}$ . A crucial symplectic operation is the one achieving the normal mode decomposition. Due to Williamson theorem [11], any  $N$ -mode Gaussian state can be symplectically diagonalized in phase space, so that its CM is brought in the form  $\nu$ , such that  $S\gamma S^T = \nu$ , with  $\nu = \text{diag} \{\nu_1, \nu_1, \dots, \nu_N, \nu_N\}$ . The set  $\{\nu_i\}$  of the positive-defined eigenvalues of  $|i\Omega\gamma|$  constitutes the symplectic spectrum of  $\gamma$  and its elements, the so-called symplectic eigenvalues, must fulfill the conditions  $\nu_i \geq 1$ , following from the uncertainty principle Eq. (2) and ensuring positivity of the density matrix  $\rho$  corresponding to  $\gamma$ .

Ideal beam splitters, phase shifters and squeezers are described by symplectic transformations. In particular, a phase-free two-mode squeezing transformation, which corresponds to squeezing the first mode (say  $i$ ) in one quadrature (say momentum,  $\hat{p}_i$ ) and the second mode (say  $j$ ) in the orthogonal quadrature (say position,  $\hat{q}_j$ ) with the same degree of squeezing  $r$ , can be represented in phase space by the symplectic transformation

$$S_{ij}(r) = \text{diag}\{\exp r, \exp -r, \exp -r, \exp r\}. \quad (3)$$

These transformations occur for instance in parametric down conversions [12]. Another important example of symplectic operation is the ideal (phase-free) beam splitter, which acts on a pair of modes  $i$  and  $j$  as [13]

$$\hat{B}_{ij}(\theta) : \begin{cases} \hat{a}_i \mapsto \hat{a}_i \cos \theta + \hat{a}_j \sin \theta \\ \hat{a}_j \mapsto \hat{a}_i \sin \theta - \hat{a}_j \cos \theta \end{cases}$$

and corresponds to a rotation in phase space of the form

$$B_{ij}(\theta) = \begin{pmatrix} \cos(\theta) & 0 & \sin(\theta) & 0 \\ 0 & \cos(\theta) & 0 & \sin(\theta) \\ \sin(\theta) & 0 & -\cos(\theta) & 0 \\ 0 & \sin(\theta) & 0 & -\cos(\theta) \end{pmatrix}. \quad (4)$$

The transmittivity  $\tau$  of the beam splitter is given by  $\tau = \cos^2(\theta)$  so that a 50:50 beam splitter ( $\tau = 1/2$ ) amounts to a phase-space rotation of  $\pi/4$ .

The combined application of a two-mode squeezing and a 50:50 beam splitter realizes the entangling *twin-beam* transformation [14]

$$T_{ij}(r) = B_{ij}(\pi/4) \cdot S_{ij}(r), \quad (5)$$

which, if applied to two uncorrelated vacuum modes  $i$  and  $j$  (whose initial CM is the identity matrix), results in the production of a pure two-mode squeezed Gaussian state with CM  $\sigma_{i,j}(r) = T_{ij}(r)T_{ij}^T(r)$  given by

$$\sigma_{i,j}(r) = \begin{pmatrix} \cosh(2r) & 0 & \sinh(2r) & 0 \\ 0 & \cosh(2r) & 0 & -\sinh(2r) \\ \sinh(2r) & 0 & \cosh(2r) & 0 \\ 0 & -\sinh(2r) & 0 & \cosh(2r) \end{pmatrix}. \quad (6)$$

The CV *entanglement* in the state  $\sigma_{i,j}(r)$  increases unboundedly as a function of  $r$ , and in the limit  $r \rightarrow \infty$  Eq. (6) approaches the (unnormalizable) Einstein-Podolski-Rosen (EPR) state [15], simultaneous eigenstate of relative position and total momentum of the two modes  $i$  and  $j$ . Concerning entanglement in general, the ‘‘positivity of partial transposition’’ (PPT) criterion states that a Gaussian CM  $\gamma$  is separable (with respect to a  $1 \times N$  bipartition) if and only if the partially transposed CM  $\tilde{\gamma}$  satisfies the uncertainty principle Eq. (2) [9, 16]. In phase space, partial transposition amounts to a mirror reflection of one quadrature associated to the single-mode partition. If  $\{\tilde{\nu}_i\}$  is the symplectic spectrum of the partially transposed CM  $\tilde{\gamma}$ , then a  $(N + 1)$ -mode Gaussian state with CM  $\gamma$  is separable if and only if  $\tilde{\nu}_i \geq 1 \forall i$ . A proper measure of CV entanglement is the logarithmic negativity  $E_N$  [17], which is readily computed in terms of the symplectic spectrum  $\tilde{\nu}_i$  of  $\tilde{\gamma}$  as

$$E_N = - \sum_{i: \tilde{\nu}_i < 1} \log \tilde{\nu}_i. \quad (7)$$

Such an entanglement monotone [18] quantifies the extent to which the PPT condition  $\tilde{\nu}_i \geq 1$  is violated. For  $1 \times N$  Gaussian states, only the smallest symplectic eigenvalue  $\tilde{\nu}_-$  of the partially transposed CM can be smaller than one [10], thus simplifying the expression of  $E_N$ : then the PPT criterion simply yields that  $\gamma$  is entangled as soon as  $\tilde{\nu}_- < 1$ , and infinite entanglement (accompanied by infinite energy in the state) is reached for  $\tilde{\nu}_- \rightarrow 0^+$ .

For  $1 \times 1$  Gaussian states  $\gamma_{i,j}$  symmetric under mode permutations, the entanglement of formation  $E_F$  is computable as well via the formula [19]

$$E_F(\gamma_{i,j}) = \max\{0, f(\tilde{\nu}_-^{i,j})\}, \quad (8)$$

with

$$f(x) = \frac{(1+x)^2}{4x} \log \frac{(1+x)^2}{4x} - \frac{(1-x)^2}{4x} \log \frac{(1-x)^2}{4x}.$$

Being a monotonically decreasing function of the smallest symplectic eigenvalue  $\tilde{\nu}_-^{i,j}$  of the partial transpose  $\tilde{\gamma}_{i,j}$  of  $\gamma_{i,j}$ , the entanglement of formation is completely equivalent to the logarithmic negativity in this case. For a two-mode state,  $\tilde{\nu}_{i,j}$  can be computed from the symplectic invariants of the state [20], and experimentally estimated with measures of global and local purities [21] (the purity  $\mu = \text{Tr} \rho^2$  of a Gaussian state  $\rho$  with CM  $\gamma$  is equal to  $\mu = (\text{Det} \gamma)^{-1/2}$ ).

### 3. Gaussian valence bond states

Let us review the basic definitions and notations for GVBS, as adopted in Ref. [4]. The so-called matrix product Gaussian states introduced in Ref. [3] are  $N$ -mode states obtained

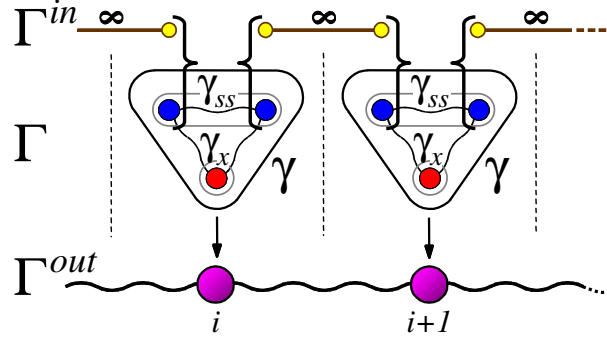


**Figure 1.** Gaussian valence bond states.  $\Gamma^{in}$  is the state of  $N$  EPR bonds and  $\gamma$  is the three-mode building block. After the EPR measurements (depicted as curly brackets), the chain of modes  $\gamma_x$  collapses into a Gaussian valence bond state with global state  $\Gamma^{out}$ . See also Ref. [4].

by taking a fixed number,  $M$ , of infinitely entangled ancillary bonds (EPR pairs) shared by adjacent sites, and applying an arbitrary  $2M \rightarrow 1$  Gaussian operation on each site  $i = 1, \dots, N$ . Such a construction, more properly definable as a “valence bond” picture for Gaussian states, can be better understood by resorting to the Jamiolkowski isomorphism between quantum operations and quantum states [22]. In this framework, one starts with a chain of  $N$  Gaussian states of  $2M + 1$  modes (the *building blocks*). The global Gaussian state of the chain is described by a CM  $\Gamma = \bigoplus_{i=1}^N \gamma^{[i]}$ . As the interest in GVBS lies mainly in their connections with ground states of Hamiltonians invariant under translation [3], we can focus on pure ( $\text{Det } \gamma^{[i]} = 1$ ), translationally invariant ( $\gamma^{[i]} \equiv \gamma \forall i$ ) GVBS. Moreover, in this work we consider single-bonded GVBS, i.e. with  $M = 1$ . This is also physically motivated in view of experimental implementations of GVBS, as more than one EPR bond would result in a building block with five or more correlated modes, which appears technologically demanding.

Under the considered prescriptions, the building block  $\gamma$  is a pure Gaussian state of three modes. As we aim to construct a translationally invariant state, it is convenient to consider a  $\gamma$  whose first two modes, which will be combined with two identical halves of consecutive EPR bonds (see Fig. 3), have the same reduced CM. This yields a pure, three-mode Gaussian building block with the property of being *bisymmetric* [23], that is with a CM invariant under permutation of the first two modes. This choice of the building block is further justified by the fact that, among all pure three-mode Gaussian states, bisymmetric states maximize the genuine tripartite entanglement [24]: no entanglement is thus wasted in the projection process. The  $6 \times 6$  CM  $\gamma$  of the building block can be written as follows in terms of  $2 \times 2$  submatrices,

$$\gamma = \begin{pmatrix} \gamma_s & \varepsilon_{ss} & \varepsilon_{sx} \\ \varepsilon_{ss}^T & \gamma_s & \varepsilon_{sx} \\ \varepsilon_{sx}^T & \varepsilon_{sx} & \gamma_x \end{pmatrix}. \quad (9)$$

The  $4 \times 4$  CM of the first two modes (each of them having reduced CM  $\gamma_s$ ) will be denoted by  $\gamma_{ss}$ , and will be regarded as the *input* port of the building block. On the other hand, the CM  $\gamma_x$  of mode 3 will play the role of the *output* port. The intermodal correlations are encoded in the off-diagonal  $\varepsilon$  matrices. Without loss of generality, we can assume  $\gamma$  to be, up to local unitary operations, in the standard form [24] with

$$\gamma_s = \text{diag}\{s, s\}, \quad \gamma_x = \text{diag}\{x, x\}, \quad (10)$$

$$\begin{aligned}\boldsymbol{\varepsilon}_{ss} &= \text{diag}\{t_+, t_-\}, \quad \boldsymbol{\varepsilon}_{sx} = \text{diag}\{u_+, u_-\}; \\ t_{\pm} &= \frac{1}{4s} \left[ x^2 - 1 \pm \sqrt{16s^4 - 8(x^2 + 1)s^2 + (x^2 - 1)^2} \right], \\ u_{\pm} &= \frac{1}{4} \sqrt{\frac{x^2 - 1}{sx}} \left[ \sqrt{(x - 2s)^2 - 1} \pm \sqrt{(x + 2s)^2 - 1} \right].\end{aligned}$$

The valence bond construction works as follows (see Fig. 3). The global CM  $\boldsymbol{\Gamma} = \bigoplus_{i=1}^N \gamma$  acts as the projector from the state  $\boldsymbol{\Gamma}^{in}$  of the  $N$  ancillary EPR pairs, to the final  $N$ -mode GVBS  $\boldsymbol{\Gamma}^{out}$ . This is realized by collapsing the state  $\boldsymbol{\Gamma}^{in}$ , transposed in phase space, with the ‘input port’  $\boldsymbol{\Gamma}_{ss} = \bigoplus_i \gamma_{ss}$  of  $\boldsymbol{\Gamma}$ , so that the ‘output port’  $\boldsymbol{\Gamma}_x = \bigoplus_i \gamma_x$  turns into the desired  $\boldsymbol{\Gamma}^{out}$ . Here collapsing means that, at each site, the two two-mode states, each constituted by one mode (1 or 2) of  $\gamma_{ss}$  and one half of the EPR bond between site  $i$  and its neighbor ( $i - 1$  or  $i + 1$ , respectively), undergo an ‘‘EPR measurement’’ i.e. are projected onto the infinitely entangled EPR state [22, 3]. An EPR pair between modes  $i$  and  $j$  can be described, see Eq. (6), as a two-mode squeezed state  $\sigma_{i,j}(r)$  in the limit of infinite squeezing ( $r \rightarrow \infty$ ). The input state is then  $\boldsymbol{\Gamma}^{in} = \lim_{r \rightarrow \infty} \bigoplus_i^N \sigma_{i,i+1}(r)$ , where we have set periodic boundary conditions so that  $N + 1 = 1$  in labeling the sites. The projection corresponds mathematically to taking a Schur complement (see Refs. [4, 3, 22] for details), yielding an output pure GVBS of  $N$  modes on a ring with a CM

$$\boldsymbol{\Gamma}^{out} = \boldsymbol{\Gamma}_x - \boldsymbol{\Gamma}_{sx}^T (\boldsymbol{\Gamma}_{ss} + \boldsymbol{\theta} \boldsymbol{\Gamma}^{in} \boldsymbol{\theta})^{-1} \boldsymbol{\Gamma}_{sx}, \quad (11)$$

where  $\boldsymbol{\Gamma}_{sx} = \bigoplus_i \gamma_{sx}$ , and  $\boldsymbol{\theta} = \bigoplus_i \text{diag}\{1, -1, 1, -1\}$  represents transposition in phase space ( $\hat{q}_i \rightarrow \hat{q}_i, \hat{p}_i \rightarrow -\hat{p}_i$ ).

Within the building block picture, the valence bond construction can be *in toto* understood as a multiple CV entanglement swapping [25], as shown in Fig. 3: the GVBS is created as the entanglement in the bonds is swapped to the chain of output modes via teleportation [26] through the input port of the building blocks. It is thus clear that at a given initialization of the output port (i.e. at fixed  $x$ ), changing the properties of the input port (i.e. varying  $s$ ), which corresponds to implementing different Gaussian projections from the ancillary space to the physical one, will affect the structure and entanglement properties of the target GVBS. This link is explored in the following section.

#### 4. Entanglement distribution

In Ref. [4] the quantum correlations of GVBS of the form Eq. (11) have been studied, and related to the entanglement properties of the building block  $\gamma$ . Let us first recall the characterization of entanglement in the latter. As a consequence of the uncertainty principle Eq. (2), the CM Eq. (9) of the building block describes a physical state if [24]

$$x \geq 1, \quad s \geq s_{\min} \equiv \frac{x+1}{2}. \quad (12)$$

Let us keep the output parameter  $x$  fixed. Straightforward applications of the PPT separability conditions, and consequent calculations of the logarithmic negativity Eq. (7), reveal that the entanglement in the CM  $\gamma_{ss}$  of the first two modes (input port) is monotonically increasing as a function of  $s$ , ranging from the case  $s = s_{\min}$  when  $\gamma_{ss}$  is separable to the limit  $s \rightarrow \infty$  when the block  $\gamma_{ss}$  is infinitely entangled. Accordingly, the entanglement between each of the first two modes  $\gamma_s$  of  $\gamma$  and the third one  $\gamma_x$  decreases with  $s$ . One can also show that the genuine tripartite entanglement in the building block increases with the difference  $s - s_{\min}$  [24]. The entanglement properties of the building block are summarized in Fig. 4.

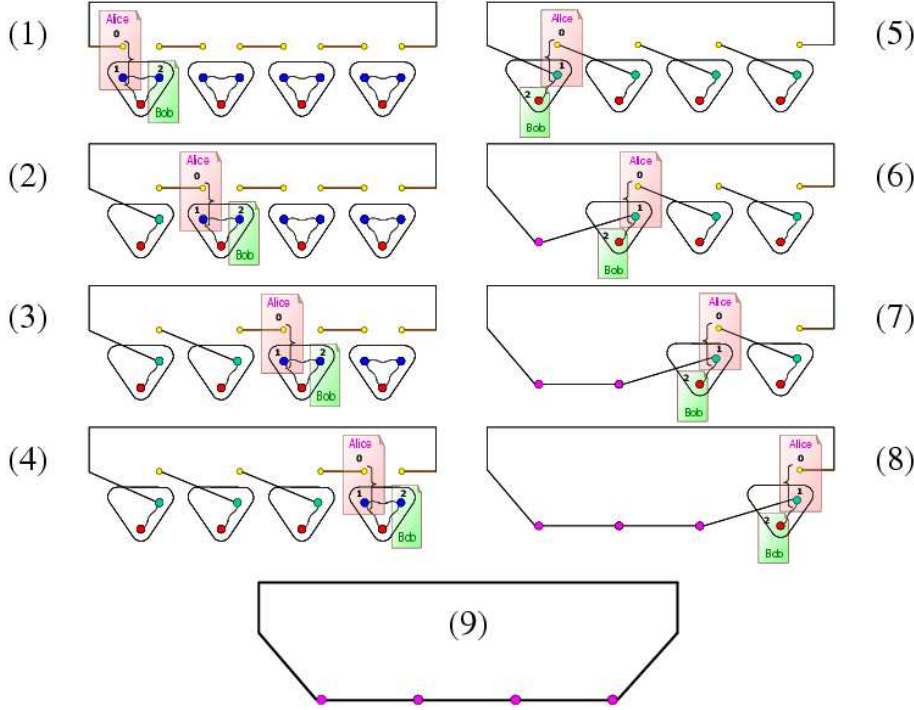


**Figure 2.** How a Gaussian valence bond state is created via continuous-variable entanglement swapping. At each step, Alice attempts to teleport her mode 0 (half of an EPR bond, depicted in yellow) to Bob, exploiting as an entangled resource two of the three modes of the building block (denoted at each step by 1 and 2). The curly bracket denotes homodyne detection, which together with classical communication and conditional displacement at Bob's side achieves teleportation. The state will be approximately recovered in mode 2, owned by Bob. Since mode 0, at each step, is entangled with the respective half of an EPR bond, the process swaps entanglement from the ancillary chain of the EPR bonds to the modes in the building block. The picture has to be followed column-wise. For ease of clarity, we depict the process as constituted by two sequences: in the first sequence [frames (1) to (4)] modes 1 and 2 are the two input modes of the building block (depicted in blue); in the second sequence [frames (5) to (8)] modes 1 and 2 are respectively an input and an output mode of the building block. As a result of the multiple entanglement swapping [frame (9)] the chain of the output modes (depicted in red), initially in a product state, is transformed into a translationally invariant Gaussian valence bond state, possessing in general multipartite entanglement among all the modes (depicted in magenta).

The main question addressed in Ref. [4] is how the initial entanglement in the building block  $\gamma$  redistributes in the Gaussian MPS  $\Gamma^{out}$ . The answer is that the more entanglement one prepares in the input port  $\gamma_{ss}$ , the longer the range of pairwise quantum correlations in the output GVBS is, as pictorially shown in Fig. 4.

In more detail, let us consider first a building block  $\gamma$  with  $s = s_{\min} = (x + 1)/2$ . In this case, a separability analysis shows that, for an arbitrary number  $N$  of modes in the GVBS chain, the target state  $\Gamma^{out}$  exhibits bipartite entanglement only between nearest neighbor modes, for any value of  $x > 1$  (for  $x = 1$  we trivially obtain a product state). In fact, each reduced two-mode block  $\gamma_{i,j}^{out}$  is separable for  $|i - j| > 1$ .

With increasing  $s$  in the choice of the building block, one finds that in the target GVBS the correlations start to extend smoothly to distant modes. A series of thresholds  $s_k$  can be

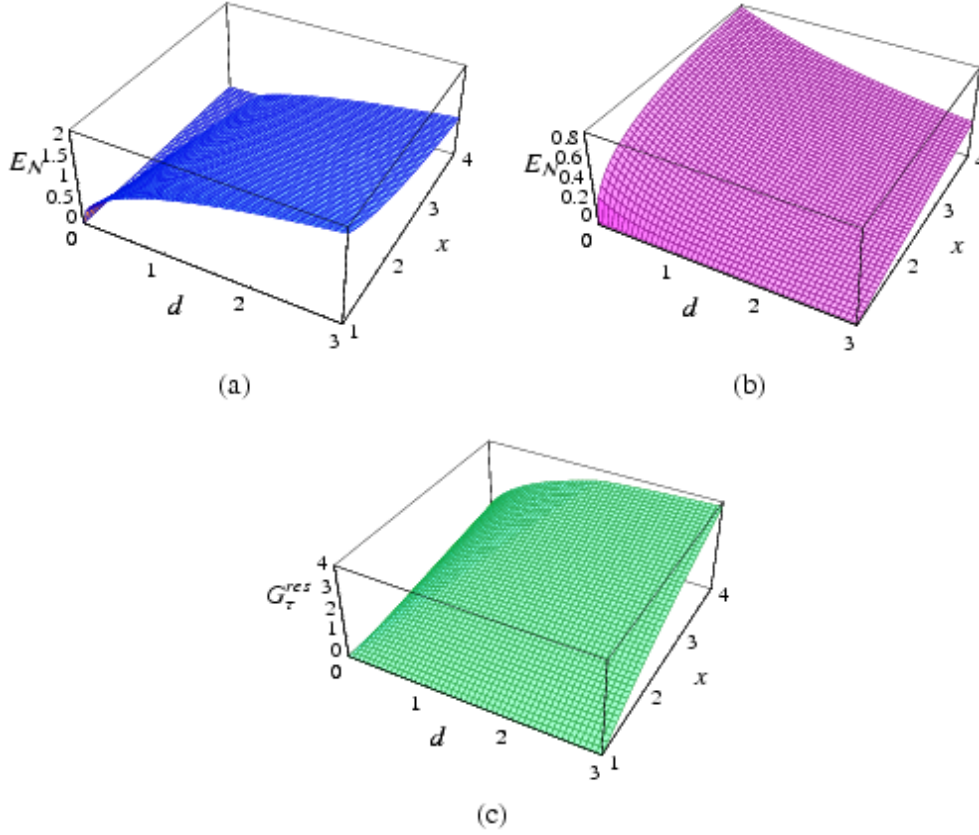


**Figure 3.** Entanglement properties of the three-mode building block  $\gamma$ , Eq. (9), of the Gaussian valence bond construction, as functions of the standard form covariances  $x$  and  $d \equiv s - s_{\min}$ . (a) Bipartite entanglement, as quantified by the logarithmic negativity, between the first two input-port modes 1 and 2; (b) Bipartite entanglement, as quantified by the logarithmic negativity, between each of the first two modes and the output-port mode 3; (c) Genuine tripartite entanglement, as quantified by the residual Gaussian contangle [27, 24], among all the three modes.

found such that for  $s > s_k$ , two given modes  $i$  and  $j$  with  $|i - j| \leq k$  are entangled. While trivially  $s_1(x) = s_{\min}$  for any  $N$  (notice that nearest neighbors are entangled also for  $s = s_1$ ), the entanglement boundaries for  $k > 1$  are in general different functions of  $x$ , depending on the number of modes. We observe however a certain regularity in the process:  $s_k(x, N)$  always increases with the integer  $k$ . Very remarkably, this means that the maximum range of bipartite entanglement between two modes, or equivalently the maximum distribution of multipartite entanglement, in a GVBS on a translationally invariant ring, is *monotonically* related to the amount of entanglement in the reduced two-mode input port of the building block [4]. Moreover, no complete transfer of entanglement to more distant modes occurs: closer sites remain still entangled even when correlations between farther pairs arise.

The most interesting feature is perhaps obtained when infinite entanglement is fed in the input port ( $s \rightarrow \infty$ ): in this limit, the output GVBS turns out to be a fully symmetric, permutation-invariant,  $N$ -mode Gaussian state. This means that each individual mode is *equally entangled* with any other, no matter how distant they are [4]. These states, being thus

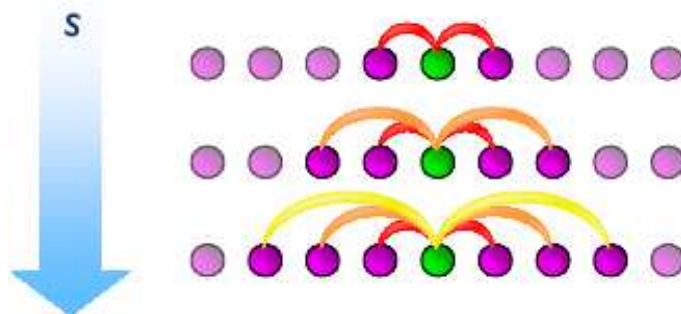


**Figure 4.** Pictorial representation of the entanglement between a probe (green) mode and its neighbor (magenta) modes on an harmonic ring with an underlying valence bond structure. As soon as the parameter  $s$  (encoding entanglement in the input port of the valence bond building block) is increased, pairwise entanglement between the probe mode and its farther and farther neighbors gradually appears in the corresponding output Gaussian valence bond states. By translational invariance, each mode exhibits the same entanglement structure with its respective neighbors. In the limit  $s \rightarrow \infty$ , every single mode becomes equally entangled with every other single mode on the ring, independently of their relative distance: the Gaussian valence bond state is in this case fully symmetric.

built by a symmetric distribution of infinite pairwise entanglement among multiple modes, achieve maximum genuine multiparty entanglement among all Gaussian states (at a given energy) while keeping the strongest possible bipartite one in any pair, a property known as monogamous but promiscuous entanglement sharing [27].

Keeping Fig. 3 in mind, we can conclude that having the two input modes initially entangled in the building blocks, increases the efficiency of the entanglement-swapping mechanism, inducing correlations between distant modes on the GVBS chain, which enable to store and distribute joint information. In the asymptotic limit of an infinitely entangled input port of the building block, the entanglement range in the target GVBS states is engineered to be maximum, and communication between any two modes, independently of their distance, is enabled nonclassically. In the next sections, we investigate the possibility of producing GVBS with linear optics, and discuss with a specific example the usefulness of such resource states for multiparty CV quantum communication protocols such as telecloning [6] and teleportation networks [13].

## 5. Optical implementation of Gaussian valence bond states

The power of describing the production of GVBS in terms of physical states, the building blocks, rather than in terms of arbitrary non-unitary Gaussian maps, lies not only in the immediacy of the analytical treatment. From a practical point of view, the recipe of Fig. 3 can be directly implemented to produce GVBS experimentally in the domain of quantum optics. We first note that the EPR measurements are realized by the standard toolbox of a beamsplitter plus homodyne detection [22], as demonstrated in several CV teleportation experiments [28].

The next ingredient to produce a  $N$ -mode GVBS is constituted by  $N$  copies of the three-mode building block  $\gamma$ . We provide here an easy scheme (see also Refs. [6, 29]) to realize bisymmetric three-mode Gaussian states of the form Eq. (9). As shown in Fig. 5(a), one can start from three vacuum modes and first apply a twin-beam operation to modes 1 and 3, characterized by a squeezing  $r_{13}$ , then apply another twin-beam operation to modes 1 and 2,

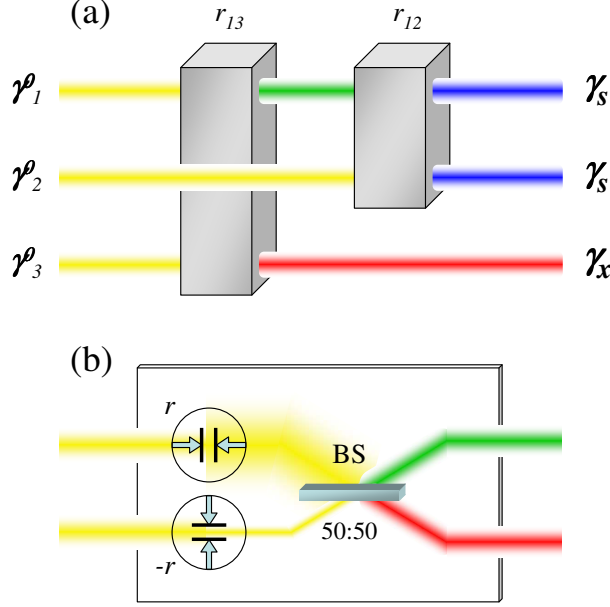


**Figure 5.** Optical production of bisymmetric three-mode Gaussian states, used as building blocks for the valence bond construction. (a) Three initial vacuum modes are entangled through two sequential twin-beam boxes, the first (parametrized by a squeezing degree  $r_{13}$ ) acting on modes 1 and 3, and the second (parametrized by a squeezing degree  $r_{12}$ ) acting on the transformed mode 1 and mode 2. The output is a pure three-mode Gaussian state whose covariance matrix is equivalent, up to local unitary operations, to the standard form given in Eq. (9). (b) Detail of the entangling twin-beam transformation. One input mode is squeezed in a quadrature, say momentum, of a degree  $r$  (this transformation is denoted by stretching arrows  $\rightarrow| \leftarrow$ ); the other input mode is squeezed in the orthogonal quadrature, say position, of the same amount (this anti-squeezing transformation is denoted by the corresponding rotated symbol). Then the two squeezed modes are combined at a 50:50 beam-splitter. If the input modes are both in the vacuum state, the output is a pure two-mode squeezed Gaussian state, with entanglement proportional to the degree of squeezing  $r$ .

parametrized by  $r_{12}$ . The symplectic operation describing the twin-beam transformation (two-mode squeezing plus balanced beam splitter) is given by Eq. (5) and pictorially represented in Fig. 5(b). The output of this optical network is a pure, bisymmetric, three-mode Gaussian state with a CM  $\gamma_B = T_{12}(r_{12})T_{13}(r_{13})T_{13}^T(r_{13})T_{12}^T(r_{12})$  of the form Eq. (9), with

$$\begin{aligned}
 \gamma_s &= \text{diag} \left\{ \frac{1}{2}e^{-2r_{12}} (e^{4r_{13}} \cosh(2r_{13}) + 1), \frac{1}{2}e^{-2r_{12}} (\cosh(2r_{13}) + e^{4r_{13}}) \right\}, \\
 \gamma_x &= \text{diag} \{ \cosh(2r_{13}), \cosh(2r_{13}) \}, \\
 \varepsilon_{ss} &= \text{diag} \left\{ \frac{1}{2}e^{-2r_{12}} (e^{4r_{13}} \cosh(2r_{13}) - 1), \frac{1}{2}e^{-2r_{12}} (\cosh(2r_{13}) - e^{4r_{13}}) \right\}, \\
 \varepsilon_{sx} &= \text{diag} \left\{ \sqrt{2}e^{r_{12}} \cosh(r_{13}) \sinh(r_{13}), -\sqrt{2}e^{-r_{12}} \cosh(r_{13}) \sinh(r_{13}) \right\}.
 \end{aligned} \tag{13}$$

By means of *local* symplectic operations (unitary on the Hilbert space), like additional single-mode squeezings, the CM  $\gamma_B$  can be brought in the standard form of Eq. (10), from which

one has

$$r_{13} = \arccos\left(\frac{\sqrt{x+1}}{\sqrt{2}}\right), \quad r_{12} = \arccos\sqrt{\frac{\sqrt{-x^3+2x^2+4s^2x-x}}{4x} + \frac{1}{2}}.$$

For a given  $r_{13}$  (i.e. at fixed  $x$ ), the quantity  $r_{12}$  is a monotonic function of the standard-form covariance  $s$ , so this squeezing parameter which enters in the production of the building block (see Fig. 5) directly regulates the entanglement distribution in the target GVBS, as discussed in Sec. 4.

The only unfeasible part of the scheme seems constituted by the ancillary EPR pairs. But are *infinitely* entangled bonds truly necessary? In Ref. [4] the possibility is considered of using a  $\Gamma^{in}$  given by the direct sum of two-mode squeezed states of Eq. (6), but with finite  $r$ . Repeating the previous analysis to investigate the entanglement properties of the resulting GVBS with finitely entangled bonds, it is found that, at fixed  $(x, s)$ , the entanglement in the various partitions is degraded as  $r$  decreases, as somehow expected. Crucially, this does not affect the connection between input entanglement and output correlation length. Numerical investigations show that, while the thresholds  $s_k$  for the onset of entanglement between distant pairs are quantitatively modified – a bigger  $s$  is required at a given  $x$  to compensate the less entangled bonds – the overall structure stays untouched. This ensures that the possibility of engineering the entanglement structure in GVBS via the properties of the building block is robust against imperfect resources, definitely meaning that the presented scheme is feasible.

Alternatively, one could from the beginning observe that the triples consisting of two projective measurements and one EPR pair can be replaced by a single projection onto the EPR state, applied at each site  $i$  between the input mode 2 of the building block and the consecutive input mode 1 of the building block of site  $i+1$  [3]. The output of all the homodyne measurements will conditionally realize the target GVBS.

## 6. Telecloning with Gaussian valence bond resources

The protocol of CV quantum *telecloning* [6] among  $N$  parties is defined as a process in which one of them (Alice) owns an unknown coherent state, and wants to distribute her state to all the other  $N - 1$  remote parties. The telecloning is achieved by a succession of standard two-party CV teleportations [26] between the sender Alice and each of the  $N - 1$  remote receivers, exploiting each time the corresponding reduced two-mode state shared as resource by the selected pair of parties. The  $1 \rightarrow 2$  CV telecloning of unknown coherent states has been recently demonstrated experimentally [7].

The no-cloning theorem [30] yields that the  $N - 1$  remote clones can resemble the original input state only to a certain extent. The *fidelity*, which quantifies the success of a teleportation experiment, is defined as  $\mathcal{F} \equiv \langle \psi^{in} | \rho^{out} | \psi^{in} \rangle$ , where “in” and “out” denote the input and the output state.  $\mathcal{F}$  reaches unity only for a perfect state transfer,  $\rho^{out} = |\psi^{in}\rangle\langle\psi^{in}|$ .

Without using entanglement, by purely classical communication, an average fidelity of  $\mathcal{F}_{cl} = 1/2$  is the best that can be achieved if the alphabet of input states includes all coherent states with even weight [31]. The sufficient fidelity criterion states that, if teleportation is performed with  $\mathcal{F} > \mathcal{F}_{cl}$ , then the two parties exploited an entangled state [31]. The converse is generally false, i.e. some entangled resources may yield lower-than-classical fidelities. In Ref. [32] it has been shown, however, that if the fidelity is optimized over all possible local unitary operations performed on the shared Gaussian resource (which preserve entanglement by definition), then it becomes *equivalent*, both qualitatively and quantitatively, to the entanglement in the resource.

Let us also recall that the fidelity of CV two-user teleportation [26] of arbitrary single-mode Gaussian states with CM  $\gamma_{in}$  (equal to the identity for coherent states) exploiting two-mode Gaussian resources with CM  $\gamma_{ab} = \begin{pmatrix} \gamma_a & \varepsilon_{ab} \\ \varepsilon_{ab}^\top & \gamma_b \end{pmatrix}$ , can be computed [33] as

$$\mathcal{F} = \frac{2}{\sqrt{\text{Det } \Sigma}}, \quad \Sigma \equiv 2\gamma_{in} + \xi\gamma_a\xi + \gamma_b + \xi\varepsilon_{ab} + \varepsilon_{ab}^\top\xi, \quad (14)$$

with  $\xi = \text{diag}\{-1, 1\}$ . We can now consider the general setting of  $1 \rightarrow N - 1$  telecloning, where  $N$  parties share a  $N$ -mode GVBS as an entangled resource, and one of them plays the role of Alice (the sender) distributing imperfect copies of unknown coherent states to all the  $N - 1$  receivers. For any  $N$ , the fidelity can be easily computed from the reduced two-mode CMs via Eq. (14) and will depend, for translationally invariant states, on the relative distance between the two considered modes.

In this work we focus on a practical example of a GVBS on a translationally invariant harmonic ring, with  $N = 6$  modes. As shown in the previous section, these states can be produced with the current optical technology. They are completely characterized, up to local unitary operations, by a  $12 \times 12$  CM analytically obtained from Eq. (11) by considering the building block in standard form Eq. (9), whose elements are algebraic functions of  $s$  and  $x$  here omitted for brevity (as no particular insight is gained from their explicit expressions). First of all we can construct the reduced CMs  $\gamma_{i,i+k}^{out}$  of two modes with distance  $k$ , and evaluate for each  $k$  the respective symplectic eigenvalue  $\tilde{\nu}_-^{i,i+k}$  of the corresponding partial transpose. The entanglement condition  $s > s_k$  will correspond to the inequality  $\tilde{\nu}_-^{i,i+k} < 1$ . With this conditions one finds that  $s_2(x)$  is the only acceptable solution to the equation:  $72s^8 - 12(x^2+1)s^6 + (-34x^4+28x^2-34)s^4 + (x^6-5x^4-5x^2+1)s^2 + (x^2-1)^2(x^4-6x^2+1) = 0$ , while for the next-next-nearest neighbors threshold one has simply  $s_3(x) = x$ . This enables us to classify the entanglement distribution and, more specifically, to observe the interaction scale in the GVBS  $\Gamma^{out}$ : as discussed in Sec. 4 and explicitly shown in Ref. [4], by increasing initial entanglement in  $\gamma_{ss}$  one can gradually switch on pairwise quantum correlations between more and more distant sites.

Accordingly, it is now interesting to test whether this entanglement is useful to achieve nonclassical telecloning towards distant receivers. In this specific instance, Alice will send two identical (approximate) clones to her nearest neighbors, two other identical clones (with in principle different fidelity than the previous case) to her next-nearest neighbors, and one final clone to the most distant site. The fidelities for the three transmissions can be computed from Eq. (14) and are plotted in Fig. 6(a). For  $s = s_{\min}$ , obviously, only the two nearest neighbor clones can be teleported with nonclassical fidelity, as the reduced states of more distant pairs are separable. With increasing  $s$  also the state transfer to more distant sites is enabled with nonclassical efficiency, but not in the whole region of the space of parameters  $s$  and  $x$  in which the corresponding two-mode resources are entangled.

As mentioned before, one can optimize the telecloning fidelity considering resources prepared in a different way but whose CM can be brought by local unitary operations (single-mode symplectic transformations) in the standard form of Eq. (11). For GVBS resources, this local-unitary freedom can be transferred to the preparation of the building block. A more general  $\gamma$  locally equivalent to the standard form given in Eq. (10), can be realized by complementing the presented state engineering scheme for the three-mode building block as in Eq. (13) [see Fig. 5(a)], with additional single-mode rotations and squeezing transformations aimed at increasing the output fidelity in the target GVBS states, while keeping both the entanglement in the building block and consequently the entanglement in the final GVBS unchanged by definition.

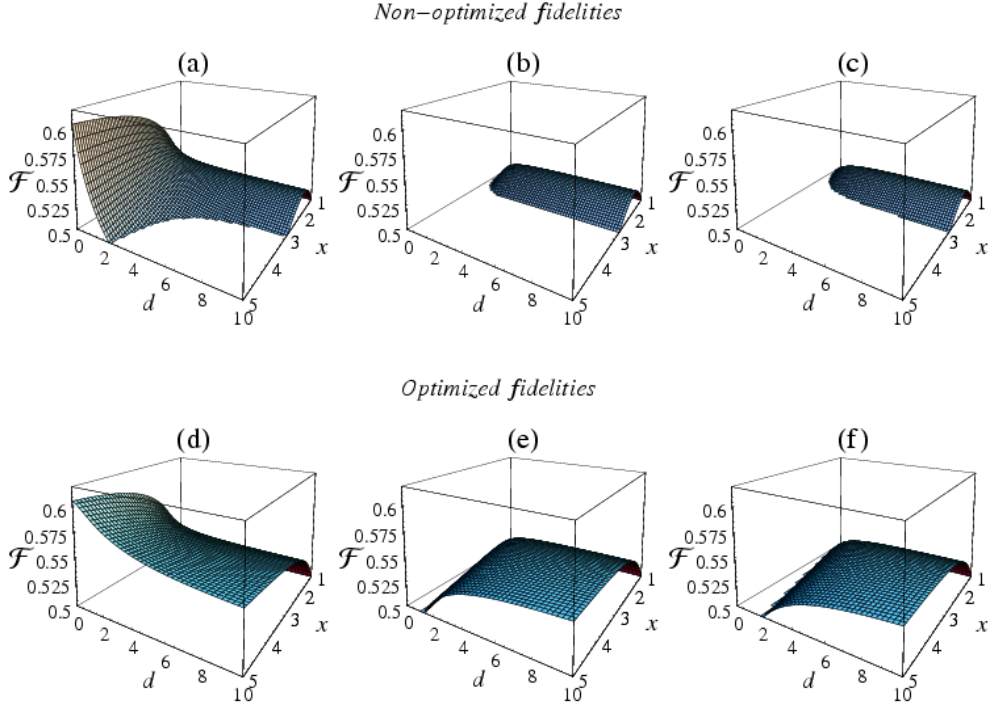


**Figure 6.**  $1 \rightarrow 5$  quantum telecloning of unknown coherent states exploiting a six-mode translationally invariant Gaussian valence bond state as a shared resource. Alice owns mode  $i$ . Fidelities  $\mathcal{F}$  for distributing clones to modes  $j$  such as  $k = |i - j|$  are plotted for  $k = 1$  [(a),(d)];  $k = 2$  [(b),(e)]; and  $k = 3$  [(c),(f)], as functions of the local invariants  $s$  and  $x$  of the building block. In the first row [(a)–(c)] the fidelities are achieved exploiting the non-optimized Gaussian valence bond resource in standard form. In the second row [(d)–(f)] fidelities optimized over local unitary operations on the resource are displayed, which are equivalent to the entanglement in the corresponding reduced two-mode states (see, as a comparison, Fig. 3 in Ref. [4]). Only nonclassical values of the fidelities ( $\mathcal{F} > 0.5$ ) are shown.

The optimal telecloning fidelity, obtained in this way exploiting the results of Ref. [32], is plotted in Fig. 6(b) for the three teleportations between modes  $i$  and  $j$  with  $k = |i - j| = 1, 2, 3$ . In this case, one immediately recovers a non-classical fidelity as soon as the separability condition  $s \leq s_k$  is violated in the corresponding resources. Moreover, the optimal telecloning fidelity at a given  $k$  is itself a quantitative measure of the entanglement in the reduced two-mode resource, being equal to [32]

$$\mathcal{F}_k^{opt} = 1/(1 + \tilde{\nu}_-^{i,i+k}), \quad (15)$$

where  $\tilde{\nu}_-^{i,i+k}$  is the smallest symplectic eigenvalue of the partially transposed CM in the corresponding bipartition. The optimal fidelity is thus completely equivalent to the entanglement of formation Eq. (8) and to the logarithmic negativity Eq. (7).

In the limit  $s \rightarrow \infty$ , as discussed in Sec. 4, the GVBS become fully permutation-invariant for any  $N$ . Consequently, the (optimized and non-optimized) telecloning fidelity for distributing coherent states is equal for any pair of sender-receiver parties. These resources are thus useful for  $1 \rightarrow N - 1$  symmetric telecloning. However, due to the monogamy constraints on distribution of CV entanglement [27], this two-party fidelity will decrease with increasing  $N$ , vanishing in the limit  $N \rightarrow \infty$  where the resources become completely separable. In this

respect, it is worth pointing out that the fully symmetric GVBS resources are more useful for teleportation networks [13, 34], where  $N - 2$  parties first perform local measurements (momentum detections) on their single-mode portion of the entangled resource to concentrate as much entanglement as possible onto the two-mode state of Alice and Bob, who can accomplish non-classical teleportation (after the outcomes of the  $N - 2$  measurements are classically communicated to Bob). In this case, the optimal fidelity of  $N$ -user teleportation network is an estimator of *multipartite* entanglement in the shared  $N$ -mode resource [32], which is indeed a GVBS obtained from an infinitely entangled building block.

## 7. Conclusion

The valence bond picture is a valuable framework to study the structure of correlations in quantum states of harmonic lattices. In fact, the motivation for such a formalism is quite different from the finite-dimensional case, where valence bond/matrix product states are useful to efficiently approximate ground states of  $N$ -body systems – generally described by a number of parameters exponential in  $N$  – with polynomial resources [2]. In continuous variable systems, the key feature of GVBS lies in the understanding of their entanglement distribution as governed by the properties of simpler structures [4]. This has also experimental implications giving a robust recipe to engineer correlations in many-body Gaussian states from feasible operations on the building blocks. We have provided a simple scheme to produce bisymmetric three-mode building blocks with linear optics, and discussed the subsequent implementation of the valence bond construction. We have also investigated the usefulness of such GVBS as resources for nonclassical communication, like telecloning of unknown coherent states to distant receivers on a harmonic ring. It would be interesting to employ the valence bond picture to describe quantum computation with continuous-variable cluster states [35], and to devise efficient protocols for its optical implementation.

## Acknowledgments

This work is supported by MIUR (Italy) and by the European Union through the Integrated Project RESQ (IST-2001-37559), QAP (IST-3-015848), SCALA (CT-015714), and SECOQC.

## References

- [1] S. L. Braunstein and P. van Loock, *Rev. Mod. Phys.* **77**, 513 (2005).
- [2] D. Perez-Garcia, F. Verstraete, M. M. Wolf, and J. I. Cirac, arXiv:quant-ph/0608197; M. Eckholt, Master Thesis (MPQ Garching, 2005), <http://www.mpg.de/Theorygroup/CIRAC/people/eckholt/diploma.pdf>, and references therein.
- [3] N. Schuch, J. I. Cirac, and M. M. Wolf, arXiv:quant-ph/0509166 (section VII).
- [4] G. Adesso and M. Ericsson, *Phys. Rev. A* **74**, 030305(R) (2006).
- [5] J. Eisert and M. B. Plenio, *Int. J. Quant. Inf.* **1**, 479 (2003); G. Adesso and F. Illuminati, arXiv:quant-ph/0510052, Chapter 1 in *Quantum Information with Continuous Variables of Atoms and Light*, N. Cerf, G. Leuchs, and E. Polzik eds. (Imperial College Press, 2007); G. Adesso and F. Illuminati, arXiv:quant-ph/0701221, *J. Phys. A* (2007), in press.
- [6] P. van Loock and S. L. Braunstein, *Phys. Rev. Lett.* **87**, 247901 (2001).
- [7] S. Koike *et al.* *Phys. Rev. Lett.* **96**, 060504 (2006).
- [8] R. Simon, E. C. G. Sudarshan, and N. Mukunda, *Phys. Rev. A* **36**, 3868 (1987).
- [9] R. Simon, *Phys. Rev. Lett.* **84**, 2726 (2000).
- [10] A. Serafini, *Phys. Rev. Lett.* **96**, 110402 (2006).
- [11] J. Williamson, *Am. J. Math.* **58**, 141 (1936).
- [12] J. Laurat *et al.*, *J. Opt. B* **7**, S577 (2005).

- [13] P. van Loock and S. L. Braunstein, Phys. Rev. Lett. **84**, 3482 (2000).
- [14] M. M. Wolf, J. Eisert and M. B. Plenio, Phys. Rev. Lett. **90**, 047904 (2003).
- [15] A. Einstein, B. Podolsky, and N. Rosen, Phys. Rev. **47**, 777 (1935).
- [16] R. F. Werner and M. M. Wolf, Phys. Rev. Lett. **86**, 3658 (2001).
- [17] G. Vidal and R. F. Werner, Phys. Rev. A **65**, 032314 (2002).
- [18] M. B. Plenio, Phys. Rev. Lett. **95**, 090503 (2005).
- [19] G. Giedke *et al.*, Phys. Rev. Lett. **91**, 107901 (2003).
- [20] G. Adesso, A. Serafini and F. Illuminati, Phys. Rev. A **70**, 022318 (2004).
- [21] G. Adesso, A. Serafini, and F. Illuminati, Phys. Rev. Lett. **92**, 087901 (2004).
- [22] J. Fiurášek, Phys. Rev. Lett. **89**, 137904 (2002); G. Giedke and J. I. Cirac, Phys. Rev. A **66**, 032316 (2002).
- [23] A. Serafini, G. Adesso and F. Illuminati, Phys. Rev. A **71**, 032349 (2005).
- [24] G. Adesso, A. Serafini and F. Illuminati, Phys. Rev. A **73**, 032345 (2006).
- [25] P. van Loock and S. L. Braunstein, Phys. Rev. A **61**, 010302(R) (2000).
- [26] L. Vaidman, Phys. Rev. A **49**, 1473 (1994); S. L. Braunstein and H. J. Kimble, Phys. Rev. Lett. **80**, 869 (1998); S. Pirandola and S. Mancini, Laser Physics **16**, 1418 (2006).
- [27] G. Adesso and F. Illuminati, New J. Phys. **8**, 15 (2006); T. Hiroshima, G. Adesso and F. Illuminati, Phys. Rev. Lett. **98**, 050503 (2007); G. Adesso and F. Illuminati, arXiv:quant-ph/0703277.
- [28] A. Furusawa *et al.*, Science **282**, 706 (1998); W. P. Bowen *et al.*, Phys. Rev. A **67**, 032302 (2003); N. Takei *et al.*, Phys. Rev. Lett. **94**, 220502 (2005).
- [29] G. Adesso, Phys. Rev. Lett. **97**, 130502 (2006); G. Adesso, A. Serafini, and F. Illuminati, New J. Phys. **9**, 60 (2007).
- [30] W. K. Wootters and W. H. Zurek, Nature **299**, 802 (1982).
- [31] S. L. Braunstein, C. A. Fuchs and H. J. Kimble, J. Mod. Opt. **47**, 267 (2000); K. Hammerer, M. M. Wolf, E. S. Polzik, and J. I. Cirac, Phys. Rev. Lett. **94**, 150503 (2005).
- [32] G. Adesso and F. Illuminati, Phys. Rev. Lett. **95**, 150503 (2005).
- [33] J. Fiurášek, Phys. Rev. A **66**, 012304 (2002).
- [34] H. Yonezawa, T. Aoki, and A. Furusawa, Nature **431**, 430 (2004).
- [35] N. C. Menicucci *et al.*, Phys. Rev. Lett. **97**, 110501 (2005); P. Van Loock, J. Opt. Soc. Am. B **24**, 340 (2007).